López-Herradón A[1,2], Lozano D[1,2,3], Portal-Núñez S[1,2], Ardura JA[1,2], Gutíerrez-Rojas I[1,4], Maycas M[1,2], Rodríguez L[3,5,6], Varela I[3,5,6], Esbrit P[1,2]

1 Laboratorio de Metabolismo Mineral y Óseo - Instituto de Investigación Sanitaria (IIS)-Fundación Jiménez Díaz - Universidad Autónoma de Madrid

2 Red Temática de Investigación Cooperativa en Envejecimiento y Fragilidad (RETICEF) - Instituto de Salud Carlos III - Madrid

3 Instituto de Investigación Hospital Universitario La Paz (IdiPAZ) de Madrid

4 Centro de Investigación Biomédica en Red de Diabetes y Enfermedades Metabólicas Asociadas (CIBERDEM) - Instituto de Salud Carlos III - Madrid

5 Instituto de Investigaciones Biomédicas "Alberto Sols" - CSIC-Universidad Autónoma de Madrid

6 Unidad 761 - Centro de Investigación Biomédica en Red de Enfermedades Raras (CIBERER) - Instituto de Salud Carlos III - Madrid

Comparison of the osteogenic actions of parathyroid hormone-related protein (PTHrP) in diabetic and insulin-like growth factor-I (IGF-I) deficient mouse models

Correspondence: Pedro Esbrit - Laboratorio de Metabolismo Mineral y Óseo - IIS-Fundación Jiménez Díaz - Avda. Reyes Católicos, 2 - 28040 Madrid (Spain)
e-mail: pesbrit@fjd.es

Date of receipt: 01/05/2014
Date of acceptance: 15/07/2014

Work scholarship with a Research Fellowship in Molecular Biology FEIOMM 2011.

Summary

Diabetes mellitus (DM) is a metabolic pathology characterised by chronic hyperglycemia due to a deficit in the production and/or action of insulin. DM, above all type I, is commonly associated with osteopenia/osteoporosis and with an increased risk of fractures. Insulin-like growth factor-I (IGF-I), a factor abundant in the bone matrix which plays a significant role in the development and maintenance of bone mass, diminishes with DM. Parathyroid hormone-related protein (PTHrP), a modulator of growth and osteoblast function, acts on osteoprogenitors, promoting osteoblast differentiation and bone regeneration. Its expression is reduced in the presence of DM. In this work we have evaluated and compared the osteogenic actions of PTHrP in mouse models with type 1 DM and IGF-I deficiency. Diabetic mice by injection of streptozotocin had a reduction in bone mass in the long bones associated with an increase in oxidised proteins and a reduction in the expression of genes related to the Wnt pathway and of β-catenin protein, as well as alterations in vertebral trabecular bone. In the mouse model with IGF-I deficit our results indicate the presence of osteopenia both in the femur (associated with an inhibition of the Wnt pathway) and the spine (L1-L5). Our findings demonstrate that the administration of PTHrP, predominantly through its N-terminal domain, modulates the canonical Wnt pathway in relation to its osteogenic actions in a diabetic situation and also, in part, in the absence of IGF-I.

Key words: *PTHrP, diabetes mellitus, IGF-I, osteopenia, Wnt pathway.*

Introduction

Diabetes mellitus (DM) is a metabolic pathology characterised by chronic hyperglycemia due to a deficit in the production and/or action of insulin, responsible for the dysfunction of organs such as the retina, the kidneys, the nervous system and the cardiovascular system[1]. Furthermore, DM is commonly associated with osteopenia/osteoporosis and with an increase in the risk of fractures, due to mechanisms only partially described[2]. DM type 1 (DM1), or insulin-dependent diabetes, is characterised by low levels of insulin and of growth factor similar to insulin type 1 (IGF-I) in the blood and is usually manifested before peak bone mass is reached, while type 2 (DM2) – associated with insulin resistance – is common in adults[3]. Skeletal changes in DM1 include: 1) a reduction in longitudinal bone growth during puberty in adolescents; 2) a reduction in bone mass in the hip, femoral head and spine in adults; 3) an increased risk of fracture; and 4) a reduction in the regenerative capacity of the bone. The characteristics of DM are compatible with a low level of bone remodelling[4-7]. Hyperglycemia induces a lower level of proliferation and function of the osteoblasts. In addition, the products of advanced glycosylation (AGEs) contribute the generation of oxidative stress, increasing bone fragility and the risk of fracture[8,9].

Among endocrine and local factors which have been shown to act on bone, insulin, produced and secreted by the β pancreatic cells and IGF-I, mainly produced in the liver but also in bone where it accumulates in the bone matrix, merit special consideration in osteopathy associated with DM[10,11]. Studies in diabetic type 1 rats indicate the role of insulin deficit in the reduction in the integrity and resistance of bone[12,13]. Furthermore, patients with DM1 have blood levels of IGF-I significantly lower in relation to those found in normal individuals or in patients with DM2[14]. It is known that systemic IGF-I plays an important role in the development and maintenance of bone mass. In fact, mice with an overall deficiency in IGF-I have a size at birth approximately 60% of that of controls, which reduces to 30% at 8 weeks, and have lower levels of bone mineralisation and of bone remodelling[15-17].

On the other hand, the protein related to parathormone (PTHrP) plays a fundamental role in the development of endochondral bone, delaying the differentiation of the chondrocyte growth plates, and acting as an important local regulator for bone remodelling in adults[18]. Homozygous Pthrp-/- mice have lethal perinatal chondrodysplasia; while heterozygous Pthrp+/- mice are viable but exhibit a significant reduction in bone mass[19]. PTHrP has a structural similarity to PTH at its N-terminal extreme, but differs completely from this hormone in the rest of its structure. The middle section and the C-terminal of PTHrP contain different singular epitopes associated with auto/paracrine and intracrine effects in different types of cells[20]. As a consequence of its post-transductional signal processing[21], PTHrP may generate different bioactive fragments: 1) an N-terminal 1-36 fragment; 2) one or many fragments from the middle region whose amino acids 88-91 and 102-106 are nuclear/nucleolar localisation domains (NLS); and 3) a C-terminal fragment which contains the sequence 107-111 known as osteostatin. Although a receptor for this C-terminal region of PTHrP has not yet been successfully isolated, it has been shown that it signals in part through the transactivation of receptor 2 of the vascular endothelial growth factor (VEGF) associated with its actions in the osteoblasts[22-24]. Previous studies have shown that PTHrP reverses the deleterious effects of DM1 on the number of osteoforming cells and the osteoblast function in a regenerating mouse tibia[25]. Furthermore, PTHrP is capable of compensating for the reduction in osteoblast differentiation and the inhibition of the signalling by means of Wnt/β-catenin – a key pathway which stimulates bone formation induced by the high levels of glucose in osteoblastic cells *in vitro*[24,26,27].

Taking into account these considerations, in this work we have evaluated and compared the consequences of insulin deficit (DM1) and IGF-I on the efficacy of PTHrP in inducing osteogenic actions in the mouse.

Materials and methods

All the studies carried out in animals were developed with the approval of the committee for experimentation and animal welfare of the Jiménez Díaz IIS-Foundation. The pain and suffering of the animals were palliated in accordance with current European regulations (Directive 2010/63/EU). In addition, the experimental design was adapted to the criteria known as 3R (replace, reduce, refine) to minimise the number of animals which still allow significant results to be obtained[28].

Model of mouse with DM1

Male CD-1 mice of 4 months of age were used (Harlan Interfauna Ibérica, Barcelona), stabilised over two weeks in the vivarium of the Jiménez Díaz IIS-Foundation. The animals had free access to water and a standard diet (8.8 g/kg of calcium and 5.9 g/kg of phosphorous; Panlab, Reus), at 22ºC with cycles of 12 hours of light and 12 hours of dark. To induce DM, the mice were injected intraperitoneally with streptozotocin (STZ) (Sigma-Aldrich, St Louis, Missouri, US), a pancreatic cytotoxin, over 5 consecutive days at a dose of 45 mg/kg body weight in a buffer solution of sodium citrate 50 mM, pH 4.5, or with a saline vehicle (controls)[25]. A week after the last injection blood glucose was measured in blood taken from the mouse tail, using a glucometer (Glucocard G+-meter, Menarini Diagnostics, Florence, Italy), those mice with glycemia ≥250 mg/dl (Figure 1A) were considered to be diabetic. Two weeks after the confirmation of DM, the mice were treated with PTHrP (1-36) (Nt) or PTHrP (107-139) (Ct) (Bachem, Bubendorf, Switzerland), 100 µg/kg in each case, or with phosphate saline buffer, pH 7.4 (PSB) (peptide vehicle) every two days by subcutaneous injection, for a total of 14 days (Figure 1A). 5 mice/group were used in each of these 4 experimental groups.

Figure 1. Description of model of mouse diabetic due to STZ. Shown are the baseline glycemia in control (Co) and diabetic (DM) mice, as well as changes in weight of each of the experimental groups. Nt, PTHrP (1-36); Ct, PTHrP (107-139). The results represent the mean ± SEM of 5 mice/group. **p<0.01 vs Co; #p<0.05; ##p<0.01 vs DM

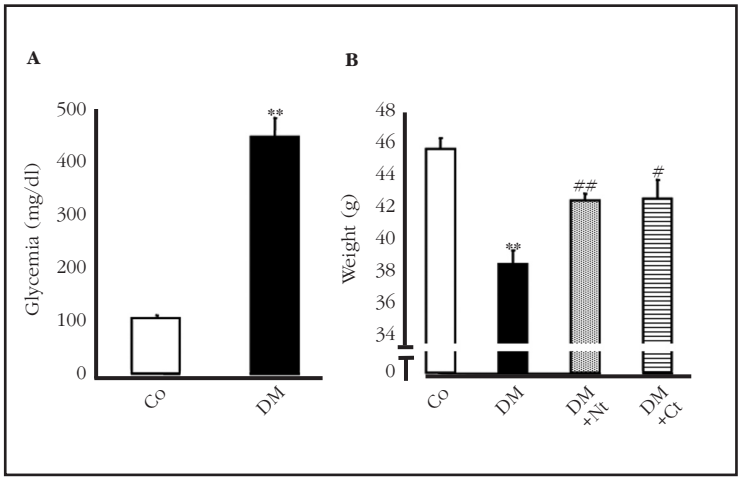

Two hours after the last injection of each treatment, the animals were weighed and then subsequently sacrificed with a mixture of ketamine (Pfizer, Madrid, Spain) 20 mg/kg and xylacine (Bayer, Kiel, Germany) 5 mg/kg (2:1, v/v). Subsequently the femurs, the tibias (discarding the fibula) and the L1-L5 vertebrae were extracted, with the adjacent muscle eliminated. The long bones were used to obtain cultures of bone marrow-derived mesenchymal cells (BMMCs), or stored (in liquid N_2) for subsequent extraction of RNA or the analysis of carbonylated proteins (at -80ºC). The vertebrae were stored at -20ºC until their incorporation into methacrylate for bone histomorphometry.

Model of mouse deficient in IGF-I

The mice with homozygous IGF-I deficiency (Igf1-null), 3 months old and with a mixed genetic background MF1/129sv, were generated after crossing heterozygous mice with a deletion in exon 4 of the Igf1[15]. The mice were genotyped using Southern Blot after the extraction of genome DNA from the tail with REDExtract-N-Amp™Tissue PCR Kit (Sigma-Aldrich) and characterised by functional criteria[29,30].

Four experimental groups were established with 6 mice per group, control and Igf1-null, treated with PTHrP (1036), PTHrP (107-111) or with PSB. The PTHrP peptides (80 µg/kg in each case) or saline vehicle were administered by subcutaneous injection every 48 hours for two weeks. This dose was chosen because similar doses of these peptides induce anabolic or antiresorptive effects, respectively, in rodents[25,29-31]. Two hours after the last injection the mice were sacrificed, as already described. The long bones were used to obtain BMMCs. The spare femurs were stored in liquid N_2 for later extraction of total RNA, and the L1-L5 vertebrae for histomorphometry.

***Ex vivo* culture of BMMCs**

To obtain the BMMCs from the femurs and tibias obtained from both animal models, the epiphysis was perforated parallel to the diaphysis with a surgical needle of 20G thickness. The marrow cavity was perfused with α-MEM culture medium supplemented with 15% foetal bovine serum, 1% penicillin-streptomycin and 2.5 µg/ml fungizone, and the bone marrow obtained. After various washes a homogenous suspension was obtained which was centrifuged at 1,500xg for 5 minutes at a cold temperature. The cell precipitate was resuspended in the aforementioned medium (without fungizone), and the number of viable cells counted (by exclusion with trypan blue) in an automatic cell counter (Countess™, Life Technologies, Paisley, United Kingdom). Subsequently, the cells were seeded at a density of 1-2, $5x10^6/cm^2$ in 6-well plates in a humid atmosphere of 5% CO_2 at 37ºC[25,32]. Osteogenic differentiation medium was added (the aforementioned medium supplemented with 50 µg/ml L-ascorbic acid and 10 nM β-glycerol phosphate) to the culture the third day after seeding. The cells were kept under these conditions for 14-16 days, with half the volume of the conditioned medium replaced every two days. During this period the BMMCs originating from diabetic or Igf1-null mice were treated *in vitro* with the PTHrP peptides (added when the medium was changed).

Bone densitometry

Using double X-ray absorptiometry (DXA) the bone mineral density (BMD; g/cm^2), the bone mineral content (BMC; g) and the % periosteal fat in the total body, the femur, the tibia and spine (vertebrae L1-L5) (regions of interest) of the anaesthetised mice were measured. The DXA was performed using a PIXIMus I instrument (GE Lunar Corp., Madison, Wisconsin, US). The instrument's programme calculates the cited parameters in different regions of the skeleton (excluding the head) with a coefficient of variation of ±2%.

Bone histomorphometry

The samples of the L1-L5 vertebrae were fixed for 24 hours in 70% ethanol and, later, dehydrated in 96% ethanol for two days and then in absolute ethanol for a further two days. Next, the samples were set in polymerised methyl-methacrylate (Merck, Whitehouse Station, New Jersey, US), following a standard protocol[34]. Then, a series of 7 µm sections were made, as close as possible to the sagittal axis of the spine with a Leica RM 2255 microtome, which were deposited on slides pretreated with Haupt's gelatine, covered with a layer of polyethylene and pressed for 20-24 hours at 60ºC. Before staining the samples were deplastici-

sed with methyl-acetate (Merck) for 15-30 minutes, followed by rehydration with ethanol at decreasing concentrations (absolute, 70% and 50%) and washed with distilled water. The von Kossa stain allows the visualisation of mineralised bone coloured black. Staining with Goldner's trichrome colours the cell nuclei blue, the osteoid borders red, and mineralised bone green. After the staining, the samples were dehydrated and mounted with DPX resin (VWR, Louvain, Belgium).

To determine the histomorphometric parameters, a micrometer coupled to a rectangular grid in the eyepiece of a microscope (Olympus BX41, Olympus, Melville, New Jersey, US) was used[32]. The following were determined: the trabecular volume as against the total bone volume (BV/TV); average trabecular thickness (Tb.Th); the number of trabeculae (Tb.N); and the trabecular separation (Tb.S), according to the criteria of the American Society for Bone and Mineral Research[33]. These parameters were evaluated independently by two observers.

Analysis of protein expression by western transference

To extract the total protein from the femur it was homogenised mechanically in a mortar. The proteins were extracted with RIPA buffer [50 mM Tris-HCl, pH 7.4, 150 mM NaCl, 1 mM EDTA, 1% Triton X-100, 1% sodium deoxycholate and 0.1% sodium dodecyl sulfate (SDS)], supplemented with protease inhibitors (Protease inhibitor cocktail P8340, Sigma-Aldrich) and phosphatases (Phosphatase inhibitor cocktail Set II, Calbiochem, La Jolla, California, US). After incubation for 30 minutes at 4ºC the samples were centrifuged at 13,000 rpm for 30 minutes, and the supernatant collected. The concentration of protein was measured using the bicinchoninic acid method (Thermo Fisher Scientific, Rockford, Illinois, US), using a bovine serum albumin curve pattern. In the protein extracts the carbonylated proteins were quantified by the derivatisation of the carbonyl groups with 2,4-dinitrophenylhydrazine (DNP-hydrazine) using the commercial test, OxyBlot protein detection kit (Millipore, Billerica, Massachusetts, US). The stable protein DNP-hydrazone obtained was detected by immunotransfer. To achieve this, the derivatized proteins (20 µg) were separated by electrophoresis in polyacrylamide-SDS gels at 12.5%, and subsequently transferred to difluoro polyvinylidene membranes (Schelider & Schuel, Keene, New Hampshire, US), followed by incubation with a primary polyclonal anti-DNP antibody and with a secondary antibody conjugated to horseradish peroxidase. The resulting bands were visualised using chemoluminescence (ECL Western Blotting Detection Reagents; GE Healthcare, Buckinghamshire, United Kingdom).

For the analysis of the proteins from the BMMCs, the protein extracts (20 µg) were separated in 8% polyacrylamide-SDS gel with 5% β-mercaptoethanol. Next, the samples were transferred to nitrocellulose membranes (Trans-Blot® SD semi-dry transfer cell, Bio-Rad, California, US). Then the membranes were blocked with skimmed milk at 2.5% in a Tri-saline buffer (Tris-HCl 50 mM, pH 7,5, NaCl 150 mM, Tween-20 al 0,1%). Subsequently, these membranes were incubated in the presence of the primary polyclonal antibody corresponding to β-catenin ([1:10000 dilution]; Abcam, Cambridge, United Kingdom) and goat anti-rabbit IgG combined with horseradish peroxidase [(1:10000 dilution); Santa Cruz, California, US]. As a loading control the expression of β-actin [(1:500 dilution); Santa Cruz] was analysed.

Analysis of gene expression using real time quantitative PCR (RT-PCR)

The total RNA was extracted from the homogenised femur (as has already been described) with Trizol (Invitrogen, Groningen, Netherlands) at 4ºC. The reverse transcription of the RNA obtained to cDNA was carried out with 0.5-1.5 µg of RNA with a high capacity cDNA reverse transcription kit (Applied Biosystems, Foster City, California, US) in a Techgene thermal cycler (Bibby Scientific Ltd., Staffordshire, United Kingdom), according to the following sequential protocol: 10 minutes at 25ºC, 120 minutes at 37ºC and 5 minutes at 85ºC. The real time PCR was carried out with: 1) specific mouse primers for the following genes of the Wnt[34] canonical pathway: Wnt3a, frizzled 2 (Fz2) and proteins related to receptors for low density lipoproteins 5 and 6 (Lrp5 and Lrp6, respectively) (Table 1), and the reaction mixture SYBR Premix Ex-Taq green polymerase (Takara, Otsu, Japan); 2) TaqMan MGB probes (Assay-by-Design™ System, Applied Biosystems) for cyclin D1 (Ccnd1) and connexin 43 (Cx43), and a reaction mixture with Premix Ex-Taq polymerase (Takara) in a ABI PRISM 7500 thermal cycler (Applied Biosystems). In parallel, ribosomal RNA 18s was amplified as normalising gene[25,31].

The dissociation curves verified the obtaining of single amplification products in the cases in which specific primers were used. The levels of expression in each experimental condition relative to the baseline control were calculated as $2^{-\Delta\Delta Ct}$ ($\Delta\Delta Ct = {}_{treatment}\Delta Ct - {}_{baseline}\Delta Ct$), as has been described earlier[27]. All the determinations were carried out in duplicate.

Statistics

The results were expressed as mean ± standard error of the mean (SEM). The comparison between various groups was carried out using the Kruskal-Wallis non-parametric test. The parametric comparison between two groups was carried out with the Student t test, while in those non-parametric comparisons the Mann Whitney test was used. Those differences with a $p<0.05$ were considered significant, The analysis was performed using the computer programme Graphpad InStat (San Diego, California, US).

Results

Osteogenic actions of PTHrP in a model of osteopenia associated with DM1 in mice

The mice, diabetic due to an injection with STZ, showed a significant reduction in body weight with respect to the controls, which was partly

Table 1. Sequence of the specific primers used for the gene amplification by real time PCR

Primer	Sequence Sense 5'-3'	Sequence Anti-sense 5'-3'
Wnt3a	GCACCACCGTCAGCAACAG	GGGTGGCTTTGTCCAGAACA
Fz2	CCGTCTCTGGATCCTCACAT	AGAAGCGCTCATTGCATACC
Lrp5	CAACGTGGACGTGTTTTATTCTTC	CAGCGACTGGTGCTGTAGTCA
Lrp6	AGATCCATCAAGTGGGTTCATGTA	GAAGCGACTTGAGCCATCCA
18s	ATGCTCTTAGCTGAGGTGCCCG	ATTCCTAGCTGCGGTATCCAGG

reversed on treatment with both PTHrP peptides (Figure 1). In these animals, the DM induced a reduction in BMD and BMC, as well as in the percentage of periosteal fat, predominantly in the long bones, alterations which were in part due to both fragments of PTHrP (Table 2).

Through histomorphometry carried out in vertebrae L1-L5 we observed that the diabetic mice showed a reduction in total trabecular volume (BV/TV), in average thickness (Tb.Th) and in the number of trabeculae (Tb.N), and an increase in trabecular separation (Tb.S), parameters which were normalised after the treatment with the PTHrP peptides (Table 3). The von Kossa stain allows the clear visualisation of these alterations in trabecular bone in the vertebrae in each of the experimental groups studied (Figure 2).

In the femur of the diabetic mice, we analysed the gene expression involved in the activation of the Wnt/β-catenin pathway. We observed that the levels of mRNA of the Wnt3a ligand, of the Fz2 receptor and of the co-receptors of Lrp5 and Lrp6, as well as those of Ccnd1 (a final target gene of this pathway) were reduced in these mice (Figure 3A). Furthermore, in the osteoprogenitors of the in the bone marrow (BMMCs) of the long bones we found a lower protein expression of β-catenin (Figure 3B). These deleterious effects of diabetic status on effectors of the Wnt/ β-catenin pathway were counteracted by the administration of PTHrP *in vivo* (above all by the N-terminal fragment) and *in vitro* (Figures 3A and 3B).

Given that DM is associated with an increase in oxidative stress, we analysed the production of oxidised proteins in the femurs of the diabetic mice[35]. These animals had an increase in oxidised proteins with respect to the controls, which showed a tendency to normalisation after treatment with PTHrP (1-36), but not with PTHrP (107-139) (Figure 3C).

Alterations in bone mass and structure associated with a deficit of IGF-I in mice and its modulation by PTHrP

The Igh1-null mice showed a significant reduction in BMD and BMC with respect to the control mice in the total body, femur and spine (L1-L5) (Figure 4A). At the end of the period of study (day 14) the Igf1-null mice showed a lower gain in bone mass in the total body, but greater in the femur and the spine which respect to the controls (Figure 4B). The treatment with both PTHrP peptides produced a significant increase in bone mass in the total body and in the femur of the Igf1-null mice (Figure 4B). Through a histomorphometric analysis, a general change was observed in the structural parameters evaluated in the L1-L5 vertebrae of the Igf1-null mice compared to the controls. Treatment with the PTHrP peptides normalised the BV/TV and the Tb.Th in these animals (Table 4).

In the Igf1-null mice we found in the femur a reduction in an initial gene and another final gene, key to the activity of the canonical Wnt, Wnt3a and Cx43 pathway, which was partially compensated for by treatment with the PTHrP peptides (Figure 5A).

In addition, we wanted to confirm whether PTHrP might exert osteogenic actions autonomously at the cellular level in the absence of IGF-1. In order to do this we used BMMC cultures from control and Igf1-null mice treated *in vitro* with both PTHrP peptides. The cultures from Igf1-null mice showed a lower capacity for mineralisation compared with the controls, which was not affected by the treatment with either PTHrP peptides (Figure 5B).

Discussion

Osteogenic effects of PTHrP in murine model of DM induced by STZ

In this study we observed a loss of weight in diabetic mice, possibly due to lipolytic action and loss of muscle induced by the drug STZ[36,37]. Using DXA we corroborated this finding with the decrease observed in the percentage of periosteal fat in the total body and the long bones of the diabetic mice. In these locations we observed, furthermore, a reduction in bone mass at 4 weeks from the instigation of DM. The treatment with PTHrP peptides compensated for this osteopenia, in accordance with earlier observations in this model of DM1 after the administration of analogues of PTH and PTHrP[25,26,38,39].

The histomorphometric analysis of the L1-L5 vertebrae showed a reduction in BV/TV and other trabecular parameters (Tb.Th, Tb.N and Tb.S) in diabetic mice, in accordance with observations in

Table 2. Values of bone mass and periosteal fat in the long bones, spine and total body of control an diabetic mice, with and without treatment PTHrP (1-36) or PTHrP (107-139)

		Control	Diabetic (DM)	DM+PTHrP (1-36)	DM+PTHrP (107-139)
Femur	BMD	0.123±0.001	0.103±0.0009**	0.106±0.001	0.119±0.001##
	BMC	0.046±0.001	0.041±0.0005**	0.042±0.0007	0.047±0.001#
	%Fat	19.45±2.376	11.56±0.409**	17.76±0.248##	13.34±0.441#
Tibia	BMD	0.084±0.002	0.076±0.0004**	0.086±0.002#	0.086±0.002##
	BMC	0.046±0.001	0.042±0.0007*	0.045±0.001#	0.046±0.0004##
	%Fat	18.94±0.909	14.98±0.485**	16.78±0.171##	18.64±0.930##
Column	BMD	0.077±0.003	0.074±0.001	0.074±0.0009	0.076±0.0007
	BMC	0.092±0.006	0.057±0.011*	0.089±0.001#	0.094±0.003#
	%Fat	18.78±1.084	11.06±0.175	10.4±0.175#	11.21±0.606
Total body	BMD	0.064±0.001	0.056±0.001**	0.067±0.001##	0.067±0.002##
	BMC	0.901±0.029	0.864±0.017	0.892±0.019	0.892±0.001
	%Fat	18.78±1.084	12.82±0.582**	13.56±0.597	12.92±2.143

BMD (g/cm^2); BMC (g). The values are the mean ± SEM of 5 mice/groups. *p<0.05; **p<0.01 vs control; #p<0.05; ##p<0.01 vs DM.

the other model of DM1 induced by STZ in mice[40]. On the other hand, recent data from a histomorphometric analysis of biopsies from the iliac crest of patients with DM1 did not indicate significant alterations in the trabecular structure compared with a healthy control group, although there is a coherent trend with results obtained in the vertebrae of diabetic mice in our study[41]. However, it is interesting to note that in these diabetic patients the samples were obtained before the appearance of complications associated with DM. Our results demonstrate the capacity of the PTHrP peptides to attenuate alterations in the vertebral trabecular structures produced by DM in mice, confirming previous findings[25,26,44].

Recent data from our group have shown changes in the Wnt/β-catenin pathways in the bone of mice with DM1 induced by STZ, associated with a reduction in sclerostin corresponding to a higher rate of osteocyte apoptosis in the tibia of these mice[42]. On the other hand, an overexpression of Sost and Dkk1 (inhibitors of the Wnt canonical pathway) was found in the tibias of diabetic mice[43]. In humans, high levels of sclerostin and a reduction in β-catenin have been found in patients with DM2[44]. The results of this work show an alteration in the expression of the canonical genes for the initial stages of the Wnt pathway in the bone of diabetic mice, in contrast with that observed in diabetic rats[43]. So, the alterations in the components of the Wnt pathway in a diabetic state appear complex and species-dependent.

The hyperglycemic state associated with DM1 causes an increase in the reactive species of oxygen (ROS), which produces an increase in protein carbonylation[35,45]. The increase observed in carbonylated proteins in the femur of diabetic mice is reduced in those treated with the N-terminal fragment of PTHrP. Similarly, the ability of PTH to reduce the production of ROS in BMMCs in the femur of old mice has been described[46]. An excess of ROS in diabetic bone affects osteoblastogenesis -causing the differentiation of the BMMCs towards adipogenesis-[47,48] and the osteoblast function, diminishing the expression of Runx2, AP and Col1α-[49], while also activating the transcription of FoxO which antagonises the canonical Wnt signalling[50]. Thus, we found a reduction in β-catenin in cultures of BMMCs originating from the long bones of diabetic mice. In this respect, in a model of non-obese diabetic mouse (similar to the model of DM1 by STZ) it was observed that there was a suppression of the PI3K/AKT pathway in osteoprogenitors cells which could contribute to the destabilisation of the β-catenin in these cells[51]. In humans, a mutation of the Sirt1 gene, directly related to the development of DM1[52], has been described, which is of interest since the SIRT1 protein promotes the translocation to the nucleus of β-catenin in osteoprogenitors cells[53].

Table 3. Alterations in histomorphometric parameters in trabecular bone (vertebrae L1-L5) of diabetic mice treated, or not, with PTHrP

Parameter	Control	Diabetic (DM)	DM + PTHrP (1-36)	DM + PTHrP (107-139)
BV/TV (%)	36.93±1.64	22.21±1.6**	37.19±2.76##	37.43±3.7##
Tb.Th. (µm)	85.49±4.53	59.91±2.24**	83.93±4.81##	88.24±2.91##
Tb. N. (mm^{-1})	2.26±0.09	1.77±0.09*	2.32±0.07##	2.30±0.15#
Tb. S. (µm)	146.93±9.71	225.97±12.07**	130.12±1.45##	130.52±12.49#

BV/TV: total trabecular volume; Tb.Th.: average trabecular thickness; Tb.N.: number of trabeculae; Tb.S.: trabecular separation. The values correspond to the mean ± SEM of 5 mice/group *p<0.05, **p<0.01 vs control; #p<0.05, ##p<0.01 vs DM.

Figure 2. Alterations in trabecular bone in the vertebrae (L1-L5) of diabetic mice with or without treatment with peptides of PTHrP. Shown are representative images obtained by optical microscope (4x) of histological sections of vertebrae of control (Co) or diabetic (DM) mice, treated, or not, with Nt (Nt) or C-terminal (Ct) PTHrP, after being set in methacrylate and with von Kossa stain, showing trabecular structure

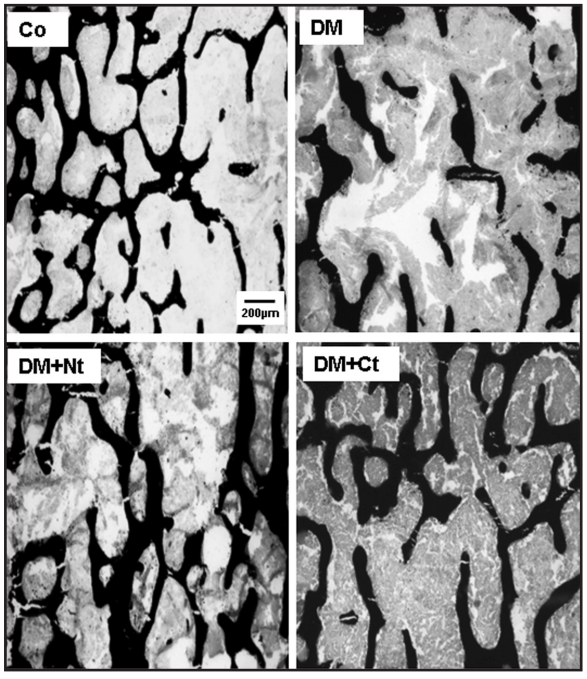

Our findings demonstrate that PTHrP (predominantly its N-terminal fragment) is capable of counteracting, at least partly, the oxidative stress and alterations in different active components of the Wnt pathway as part of its osteogenic actions in diabetic bone.

Osteogenic effects of PTHrP (1-36) and osteostatin in a mouse model deficient in IGF-I

The IGF system plays a determining role in the regulation of somatic growth. It has been suggested that a reduction in the production and/or activity of IGF-I may contribute to the loss of bone mass associated with age[54]. However, it has also been speculated that this reduction would cause a lower level of bone remodelling and thus preserve the solidity of the long bones in this situation[55]. IGF-I increases the periosteal bone formation, but its effects in trabecular bone are variable[16,56,57]. The differences observed in the skeletons of mice deficient in IGF-I could be the consequence of the dual effect of this factor on osteoblastogenesis and osteoclastogenesis and its relative impact according to bone location[16].

In this work we used a mouse model deficient in the expression of Igf1 which shows significant alterations in the mass and structure of the trabecular bone in the vertebrae, compensated for in part by both PTHrP peptides. It is worth mentioning the anabolic effects of PTH observed in the trabecular bone of mice deficient in IGF-I synthesised in the liver[58]. The low resorptive activity associated with IGF-I deficiency could facilitate the manifestation of an anabolic action of PTHrP in trabecular bone[16,59]. In fact, anabolic effects of both N- and C-terminal PTHrP fragments have been described in trabecular bone in the femur of mice diabetic due to STZ, with low levels of bone remodelling[25,26].

We observed significant changes in various components of the canonical Wnt pathway compatible with alterations in bone remodelling in mice deficient in IGF-I. Previous data in mice with a deficit of IGF-I in osteocytes showed a marked deficiency in bone development and in the response to mechanical stimulation, associated with a deficient activation of the Wnt pathway[60,61]. In our study we found that the administration of PTHrP (1-36) or osteostatin partly corrects the alterations observed in the canonical Wnt pathway in mice deficient in IGF-I. Similarly, as our data show, both PTHrP (1-36) and the native C-terminal fragment of PTHrP (107-139) act on this metabolic pathway in mice diabetic due to STZ[25,26,42].

In addition, we found that the BMMCs of mice with IGF-I deficit showed lower osteogenic capa-

Table 4. Alterations in histomorphometric parameters in the L1-L5 vertebrae of Igf1-null mice treated, or not, with PTHrP

Parameter	Control	Igf1-null	Igf1-null+Nt	Igf1-null+Ost
BV/TV (%)	26.1±1.5	16.5±0.9**	22.6±3.3#	22.85±0.2#
Tb. Th (μm)	54.5±2	45.9±1.8**	65.4±3**,##	52.5±2.5#
Tb. Sp (μm)	156±6.8	214.7±19.3**	230.6±27.9**	213.2±9.24**
Tb. N (1/mm)	4.7±0.1	3.7±0.2**	3.4±0.3**	3.6±0.23**

BV/TV: total trabecular volume/total volume; Tb.Th: trabecular thickness; Tb.N: number of trabeculae; Tb.Sp: trabecular separation. Nt, PTHrP (1-36); Ost, osteostatin. The values are the mean ± SEM of 6 mice/group. **p<0.01 vs control; #p<0.05; ##p<0.01 vs Igf1-null.

city than the control mice. A similar result was obtained in mice with a deficit of Igf1r in mature osteoblasts[62,63]. Furthermore, these BMMCs showed a lack of response to PTHrP *in vitro*, indicating that IGF-I is essential for the action of PTHrP on these osteoprogenitor cells.

These findings, overall, show that PTHrP, predominantly through its N-terminal domain, is capable of modulating the canonical Wnt pathway in relation to its osteogenic actions in a diabetic situation. Furthermore, a functional IGF-I system is necessary for at least a part of the osteogenic actions of PTHrP (1-36) and osteostatin in the mouse skeleton.

Acknowledgements: The human PTHrP (1-36) was generously donated by Drs A.F Stewart and A.García Ocaña (Faculty of Medicine of the University of Pittsburg, Pennsylvania, US).

Other funding: This work has also been funded by grants from the Ministry of Education and Culture (SAF2005-05254), the Carlos III Institute of Health (PI050117, PI080922, PI11/00449, RD06/0013/1002 and RD12/0043/0008) and the Ministry of Science and Innovation (SAF2011-24391). AL-H and MM were awarded grants by the Conchita Rábago Foundation, as well as by the Ministry of Education FPU programme (AP2009-1871) (AL-H) and the Ministry for the Economy and Competitiveness (FI12/00458) (MM). LR-de la R has contract with CIBERER. SP-N and DL have post-doctoral contracts with RETICEF (RD06/0013/1002 and RD12/0043/0008) and the Autonomous Community of Madrid (S-2009/Mat-1472), respectively.

Figure 3. Effect of PTHrP on the Wnt/β-catenin pathway in the long bones of diabetic mice. (A) Changes in the expression of genes related to the Wnt canonical pathway (analysed by real time PCR) in the femurs of control (Co) and diabetic (DM) mice, treated or not with the N-terminal (Nt) or C-terminal (Ct) fragments of PTHrP. (B) Representative autoradiography of the changes in the expression of β-catenin in BMMCs extracted from the femurs and tibias of these mice, cultivated for 14 days in an estrogenic medium, in the presence or absence of each of the PTHrP peptides (100 nM). The average relative intensities of the β-catenin signal, normalised to that of β-actin for each of the experimental condition, to the control in a representative experiment, are shown. (C) The effect of PTHrP on the oxidation of proteins in diabetic mice. Measure of the carbonylated proteins in the femur of control and diabetic mice, treated or not with the PTHrP peptides. The results in A and C correspond to the mean ± SEM of the values obtained in 5 mice in each experimental condition. *p<0.05, **p<0.01 vs Co; #p<0.05, ##p<0.01 vs DM

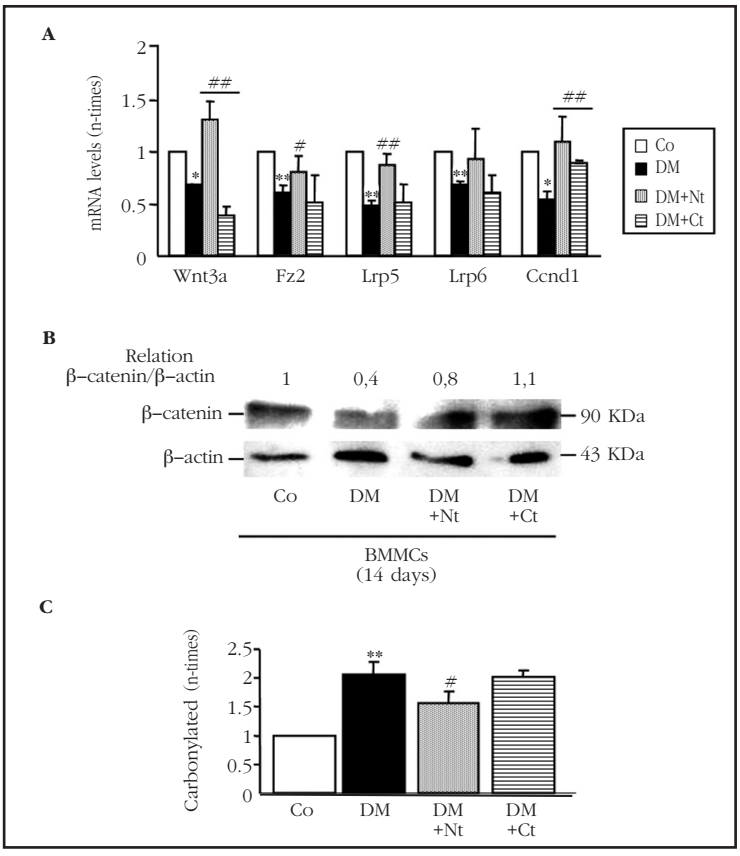

Figure 4. Description of the changes in bone mass of Igf1-null mice treated or not with PTHrP. (A) Values of BMD and BMC of control (Co) and Igf1-null mice at the start of the study (day 0) in total body, femur and spine. (B) Increases (**Δ**) in % of the values of BMD and BMC since the start (day 0) until the end of the study (day 14) for each of the genotypes, and effect of treatment with N-terminal PTHrP (Nt) or with osteostatin (Ost) (or vehicle, V). The values correspond to the means ± SEM of 6 mice for each experimental condition. **p<0.01 vs Co (A); *p<0.05 vs V-control; #p<0.05; ##p<0.01 vs V-Igf1-null (B)

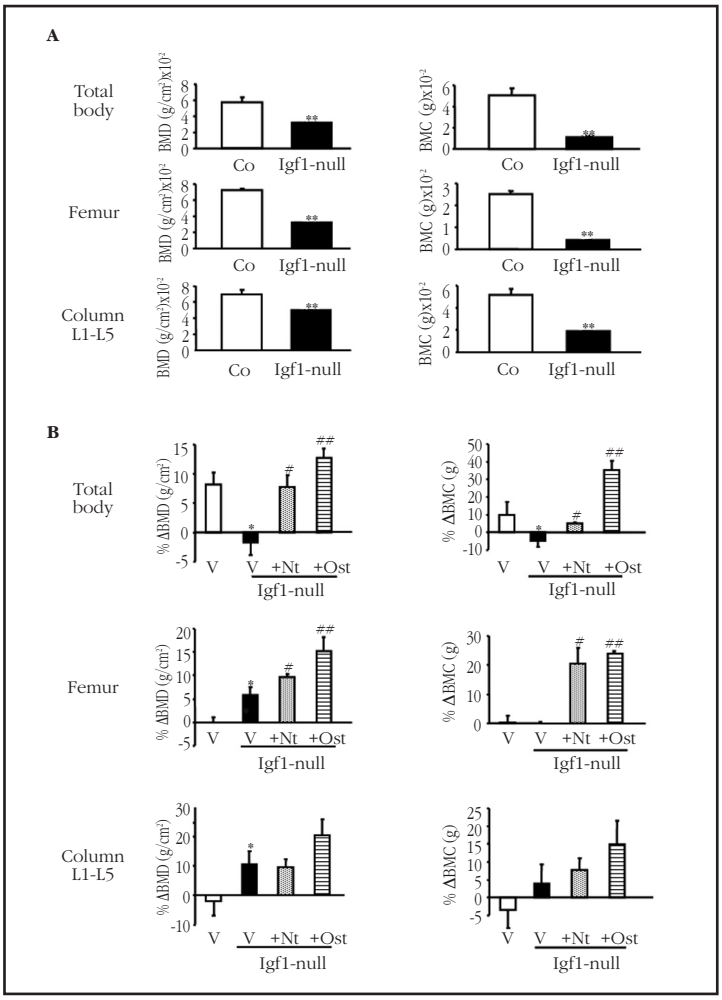

Declaration of interests: The authors declare that they have no conflicts of interest.

Bibliography

1. Association AD. Diagnosis and classification of diabetes mellitus. Diabetes Care 2009;37 (Suppl1):S81-90.
2. Wongdee K, Charoenphandhu N. Osteoporosis in diabetes mellitus: Possible cellular and molecular mechanisms. World J Diabetes 2011;2:41-8.
3. Adami S. Bone health in diabetes: considerations for clinical management. Curr Med Res Opin 2009;25:1057-72.
4. McCabe LR. Understanding the pathology and mechanisms of type I diabetic bone loss. J Cell Biochem 2007;102:1343-57.
5. Rakel A, Sheehy O, Rahme E, Le Lorier J. Osteoporosis among patients with type 1 and type 2 diabetes. Diabetes Metab 2008;34:193-205.
6. Botolin S, Faugere MC, Malluche H, Orth M, Meyer R, McCabe LR. Increased bone adiposity and peroxisomal proliferator-activated receptor-gamma2 expression in type I diabetic mice. Endocrinology 2005;146:3622-31.
7. Starup-Linde J. Diabetes, biochemical markers of bone turnover, diabetes control, and bone. Front Endocrinol (Lausanne) 2013;4:21.
8. Yamagishi S. Role of advanced glycation end products (AGEs) in osteoporosis in diabetes. Curr Drug Targets 2011;12:2096-102.
9. Saito M, Marumo K. Bone quality in diabetes. Front Endocrinol (Lausanne) 2013;4:72.
10. Carney EF. Bone: modulation of IGF-1 might prevent osteoporosis. Nat Rev Rheumatol 2012;8:440.
11. Thrailkill KM, Lumpkin CK, Jr., Bunn RC, Kemp SF, Fowlkes JL. Is insulin an anabolic agent in bone? Dissecting the diabetic bone for clues. Am J Physiol Endocrinol Metab 2005;289:E735-45.
12. Einhorn TA, Boskey AL, Gundberg CM, Vigorita VJ, Devlin VJ, Beyer MM. The mineral and mechanical properties of bone in chronic experimental diabetes. J Orthop Res 1988;6:317-23.
13. Hou JC, Zernicke RF, Barnard RJ. Effects of severe diabetes and insulin on the femoral neck of the immature rat. J Orthop Res 1993;11:263-71.
14. Jehle PM, Jehle DR, Mohan S, Bohm BO. Serum levels of insulin-like growth factor system components and relationship to bone metabolism in Type 1 and Type 2 diabetes mellitus patients. J Endocrinol 1998;159:297-306.
15. Liu JP, Baker J, Perkins AS, Robertson EJ, Efstratiadis A. Mice carrying null mutations of the genes encoding insulin-like growth factor I (Igf-1) and type 1 IGF receptor (Igf1r). Cell 1993;75:59-72.
16. Bikle DD, Majumdar S, Laib A, Powell-Braxton L, Rosen C, Beamer W, et al. The skeletal structure of insulin-like growth factor I-deficient mice. J Bone Miner Res 2001;16:2320-9.
17. Wang Y, Nishida S, Sakata T, Elalieh HZ, Chang W, Halloran BP, et al. Insulin-like growth factor-I is essential for embryonic bone development. Endocrinology 2006;147:4753-61.
18. Kartsogiannis V, Moseley J, McKelvie B, Chou ST, Hards DK, Ng KW, et al. Temporal expression of PTHrP during endochondral bone formation in mouse and intramembranous bone formation in an in vivo rabbit model. Bone 1997;21:385-92.
19. Amizuka N, Karaplis AC, Henderson JE, Warshawsky H, Lipman ML, Matsuki Y, et al. Haploinsufficiency of parathyroid hormone-related peptide (PTHrP) results in abnormal postnatal bone development. Dev Biol 1996;175:166-76.
20. McCauley LK, Martin TJ. Twenty-five years of PTHrP progress: from cancer hormone to multifunctional cytokine. J Bone Miner Res 2013;27:1231-9.
21. Orloff JJ, Reddy D, de Papp AE, Yang KH, Soifer NE, Stewart AF. Parathyroid hormone-related protein as a prohormone: posttranslational processing and receptor interactions. Endocr Rev 1994;15:40-60.
22. de Gortazar AR, Alonso V, Álvarez-Arroyo MV, Esbrit P. Transient exposure to PTHrP (107-139) exerts anabolic effects through vascular endothelial growth factor receptor 2 in human osteoblastic cells in vitro. Calcif Tissue Int 2006;79:360-9.
23. Alonso V, de Gortazar AR, Ardura JA, Andrade-Zapata I, Álvarez-Arroyo MV, Esbrit P. Parathyroid hormone-related protein (107-139) increases human osteoblastic cell survival by activation of vascular endothelial growth factor receptor-2. J Cell Physiol 2008;217:717-27.
24. García-Martín A, Acitores A, Maycas M, Villanueva-Peñacarrillo ML, Esbrit P. Src kinases mediate VEGFR2 transactivation by the osteostatin domain of PTHrP to modulate osteoblastic function. J Cell Biochem 2013;114:1404-13.
25. Lozano D, de Castro LF, Dapia S, Andrade-Zapata I,

Manzarbeitia F, Álvarez-Arroyo MV, et al. Role of parathyroid hormone-related protein in the decreased osteoblast function in diabetes-related osteopenia. Endocrinology 2009;150:2027-35.
26. Lozano D, Fernández-de-Castro L, Portal-Núñez S, López-Herradón A, Dapia S, Gómez-Barrena E, et al. The C-terminal fragment of parathyroid hormone-related peptide promotes bone formation in diabetic mice with low-turnover osteopaenia. Br J Pharmacol 2011;162:1424-38.
27. López-Herradón A, Portal-Núñez S, García-Martín A, Lozano D, Pérez-Martínez FC, Ceña V, et al. Inhibition of the canonical Wnt pathway by high glucose can be reversed by parathyroid hormone-related protein in osteoblastic cells. J Cell Biochem 2013;114:1908-16.
28. Russell WMS, Burch RL. The principles of humane experimental technique. 1959, London: Methuen and Co. ltd.
29. Rihani-Basharat S, Lewinson D. PTHrP(107-111) inhibits in vivo resorption that was stimulated by PTHrP(1-34) when applied intermittently to neonatal mice. Calcif Tissue Int 1997;61:426-8.
30. de Castro LF, Lozano D, Dapia S, Portal-Núñez S, Caeiro JR, Gómez-Barrena E, et al. Role of the N- and C-terminal fragments of parathyroid-hormone-related protein as putative therapies to improve bone regeneration under high glucocorticoid treatment. Tissue Eng Part A 2010;16:1157-68.
31. de Castro LF, Lozano D, Portal-Núñez S, Maycas M, De la Fuente M, Caeiro JR, et al. Comparison of the skeletal effects induced by daily administration of PTHrP (1-36) and PTHrP (107-139) to ovariectomized mice. J Cell Physiol 2012;227:1752-60.
32. Serrano S, Aubia J, Mariñoso M. Patología ósea metabólica. 1990, Barcelona: Sandoz S.A.E.
33. Dempster DW, Compston JE, Drezner MK, Glorieux FH, Kanis JA, Malluche H, et al. Standardized nomenclature, symbols, and units for bone histomorphometry: a 2012 update of the report of the ASBMR Histomorphometry Nomenclature Committee. J Bone Miner Res 2013;28:2-17.
34. Logan CY, Nusse R. The Wnt signaling pathway in development and disease. Annu Rev Cell Dev Biol 2004;20:781-810.
35. Dalle-Donne I, Rossi R, Giustarini D, Milzani A, Colombo R. Protein carbonyl groups as biomarkers of oxidative stress. Clin Chim Acta 2003;329:23-38.
36. Szkudelski T, Szkudelska K. Streptozotocin induces lipolysis in rat adipocytes in vitro. Physiol Res 2002;51:255-9.
37. Kelleher AR, Fairchild TJ, Keslacy S. STZ-induced skeletal muscle atrophy is associated with increased p65 content and downregulation of insulin pathway without NF-kappaB canonical cascade activation. Acta Diabetol 2010;47:315-23.
38. Suzuki K, Miyakoshi N, Tsuchida T, Kasukawa Y, Sato K, Itoi E. Effects of combined treatment of insulin and human parathyroid hormone(1-34) on cancellous bone mass and structure in streptozotocin-induced diabetic rats. Bone 2003;33:108-14.
39. Motyl KJ, McCauley LK, McCabe LR. Amelioration of type I diabetes-induced osteoporosis by parathyroid hormone is associated with improved osteoblast survival. J Cell Physiol 2012;227:1326-34.
40. Illien-Junger S, Grosjean F, Laudier DM, Vlassara H, Striker GE, Iatridis JC. Combined anti-inflammatory and anti-AGE drug treatments have a protective effect on intervertebral discs in mice with diabetes. PLoS One 2013;8:e64302.
41. Armas LA, Akhter MP, Drincic A, Recker RR. Trabecular bone histomorphometry in humans with Type 1 Diabetes Mellitus. Bone 2012;50:91-6.
42. Portal-Núñez S, Lozano D, de Castro LF, de Gortazar AR, Nogués X, Esbrit P. Alterations of the Wnt/beta-catenin pathway and its target genes for the N- and C-terminal domains of parathyroid hormone-related protein in bone from diabetic mice. FEBS Lett 2010;584:3095-100.

Figure 5. (A) Changes in factors related to the canonical Wnt pathway in Igf1-null mice, treated or not with PTHrP. Gene expressions (evaluated by real time PCR) of Wnt3a and Cx43 in the femurs of these mice, and the effect of treatment with PTHrP (1-36) (Nt) or osteostatin (Ost) (or vehicle, V). The values represent the means ± SEM of 6 mice/group. *p<0.05 vs V; #p<0.05; ##p<0.01 vs V-Igf1-null. (B) Alteration in the mineralising capacity of BMMCs in Igf1-null mice. The BMMCs of 2 Co mice or 5 gf1-null mice were cultivated for 16 days, with or without (saline vehicle, V) PTHrP (1-36) (Nt) or osteostatin (Ost) (100 nM). The mineralisation was evaluated by staining with alizarin red S (representative images are shown). The values represent the means ± SEM for 7 culture wells per experimental condition. **p<0.01 vs V-control

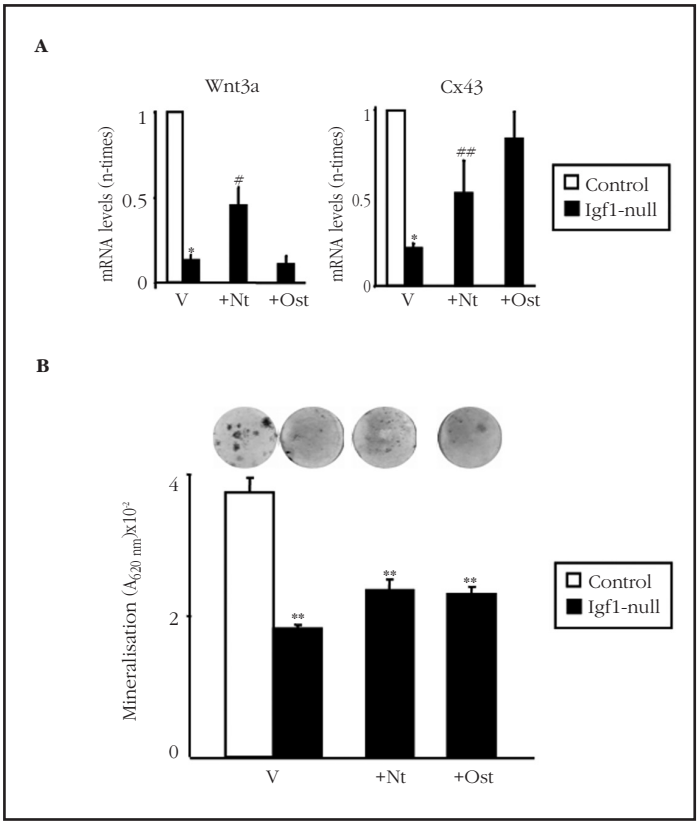

43. Hie M, Iitsuka N, Otsuka T, Tsukamoto I. Insulin-dependent diabetes mellitus decreases osteoblastogenesis associated with the inhibition of Wnt signaling through increased expression of Sost and Dkk1 and inhibition of Akt activation. Int J Mol Med 2011;28:455-62.
44. Gaudio A, Privitera F, Battaglia K, Torrisi V, Sidoti MH, Pulvirenti I, et al. Sclerostin levels associated with inhibition of the Wnt/beta-catenin signaling and reduced bone turnover in type 2 diabetes mellitus. J Clin Endocrinol Metab 2012;97:3744-50.
45. Wong CM, Marcocci L, Liu L, Suzuki YJ. Cell signaling by protein carbonylation and decarbonylation. Antioxid Redox Signal 2010;12:393-404.
46. Jilka RL, Almeida M, Ambrogini E, Han L, Roberson PK, Weinstein RS, et al. Decreased oxidative stress and greater bone anabolism in the aged, when compared to the young, murine skeleton with parathyroid hormone administration. Aging Cell 2010;9:851-67.
47. Yamaguchi M. Bone Marrow Mesenchymal Stem Cell Differentiation: Involvement in Osteoporosis with Obesity and Diabetes. J Bone Marrow Res 2013;1:e107.
48. Li W, Hu W, Ho F. High glucose induced bone loss via attenuating the proliferation and osteoblastogenesis and enhancing adipogenesis of bone marrow mesenchymals-tem cells. Biomed Eng Appl Basis Commun 2013;25:1-15.
49. Graves D, Alblowi J, Paglia D, O'Connor J, Lin S. Impact of diabetes on fracture healing. J Exp Clin Med 2011;3:3-8.

50. Almeida M, Han L, Martin-Millan M, O'Brien CA, Manolagas SC. Oxidative stress antagonizes Wnt signaling in osteoblast precursors by diverting beta-catenin from T cell factor- to forkhead box O-mediated transcription. J Biol Chem 2007;282:27298-305.
51. Li L, Xia Y, Wang Z, Cao X, Da Z, Guo G, et al. Suppression of the PI3K-Akt pathway is involved in the decreased adhesion and migration of bone marrow-derived mesenchymal stem cells from non-obese diabetic mice. Cell Biol Int 2011;35:961-6.
52. Hughes JW, Herold KC. Novel SIRT1 mutation linked to autoimmune diabetes in humans. Cell Metab 2013;17:311-2.
53. Simic P, Zainabadi K, Bell E, Sykes DB, Saez B, Lotinun S, et al. SIRT1 regulates differentiation of mesenchymal stem cells by deacetylating beta-catenin. EMBO Mol Med 2013;5:430-40.
54. Cao JJ, Kurimoto P, Boudignon B, Rosen C, Lima F, Halloran BP. Aging impairs IGF-I receptor activation and induces skeletal resistance to IGF-I. J Bone Miner Res 2007;22:1271-9.
55. Courtland HW, Kennedy OD, Wu Y, Gao Y, Sun H, Schaffler MB, et al. Low levels of plasma IGF-1 inhibit intracortical bone remodeling during aging. Age (Dordr) 2012;35:1691-703.
56. Yakar S, Courtland HW, Clemmons D. IGF-1 and bone: New discoveries from mouse models. J Bone Miner Res 2010;25:2543-52.
57. Sakata T, Wang Y, Halloran BP, Elalieh HZ, Cao J, Bikle DD. Skeletal unloading induces resistance to insulin-like growth factor-I (IGF-I) by inhibiting activation of the IGF-I signaling pathways. J Bone Miner Res 2004;19:436-46.
58. Yakar S, Bouxsein ML, Canalis E, Sun H, Glatt V, Gundberg C, et al. The ternary IGF complex influences postnatal bone acquisition and the skeletal response to intermittent parathyroid hormone. J Endocrinol 2006;189:289-99.
59. Bikle DD, Sakata T, Leary C, Elalieh H, Ginzinger D, Rosen CJ, et al. Insulin-like growth factor I is required for the anabolic actions of parathyroid hormone on mouse bone. J Bone Miner Res 2002;17:1570-8.
60. Sheng MH, Zhou XD, Bonewald LF, Baylink DJ, Lau KH. Disruption of the insulin-like growth factor-1 gene in osteocytes impairs developmental bone growth in mice. Bone 2013;52:133-44.
61. Lau KH, Baylink DJ, Zhou XD, Rodriguez D, Bonewald LF, Li Z, et al. Osteocyte-derived insulin-like growth factor I is essential for determining bone mechanosensitivity. Am J Physiol Endocrinol Metab 2013;305:E271-81.
62. Wang Y, Nishida S, Boudignon BM, Burghardt A, Elalieh HZ, Hamilton MM, et al. IGF-I receptor is required for the anabolic actions of parathyroid hormone on bone. J Bone Miner Res 2007;22:1329-37.
63. Zhang M, Xuan S, Bouxsein ML, von Stechow D, Akeno N, Faugere MC, et al. Osteoblast-specific knockout of the insulin-like growth factor (IGF) receptor gene reveals an essential role of IGF signaling in bone matrix mineralization. J Biol Chem 2002;277:44005-12.